Available online at www.sciencedirect.com
SCIENCE DIRECT®
Marine Chemistry 84 (2004) 161–179
MARINE CHEMISTRY
www.elsevier.com/locate/marchem

Processes regulating oxygen and carbon dioxide in surface waters west of the Antarctic Peninsula

Christopher J. Carrillo[a,b], Raymond C. Smith[b,*], David M. Karl[a]

[a] School of Ocean and Earth Science and Technology, University of Hawaii, Honolulu, HI 96822, USA
[b] Institute for Computational Earth System Sciences, University of California-Santa Barbara, Santa Barbara, CA 93106, USA

Received 23 September 2002; received in revised form 11 June 2003; accepted 17 July 2003

Abstract

Geographic surveys of oxygen (O_2) and carbon dioxide (CO_2) concentrations in surface waters west of the Antarctic Peninsula show the large temporal and spatial variability predicted for polar regions with winter ice cover and vernal phytoplankton blooms. The saturation states of surface seawater fugacity of carbon dioxide ($fCO_{2\{Sat\}}$) ranged from 27% to 112% relative to the atmosphere and oxygen saturation states ($O_{2\{Sat\}}$) ranged from 81% to 157% of the corresponding air-saturated values. Areas of O_2 supersaturation and fCO_2 undersaturation occurred mostly in coastal waters and were correlated with increases in chlorophyll *a* indicating a biological influence. Net community production (NCP) showed offshore to onshore gradients with O_2 production as high as 23.8 mmol O_2 m^{-3} day^{-1} and CO_2 consumption as high as 19.2 mmol C m^{-3} day^{-1} within coastal areas. Areas of surface water O_2 and fCO_2 supersaturation were found further offshore, suggesting heating as a locally significant process. Areas of fCO_2 supersaturation and O_2 undersaturation were also found further offshore suggesting upwelling as a source of the CO_2-enriched waters. Finally, within selected coastal areas, O_2 and fCO_2 were undersaturated suggesting cooling as a locally significant process. The seasonal phasing of biological, chemical and physical processes can help explain the temporal and regional variability that was observed in the saturation states of O_2 and fCO_2.
© 2003 Elsevier B.V. All rights reserved.

Keywords: Southern ocean; Carbon dioxide; Oxygen; Gas flux; Net community production

1. Introduction

The Southern Ocean comprises 22% (77×10^6 km^2) of the total global ocean surface, but remains poorly sampled relative to more accessible oceanic habitats (Tomczak and Godfrey, 1994). Open ocean areas in the Southern Ocean have high nutrient concentrations but relatively low standing stocks of phytoplankton and low rates of primary production (Holm-Hansen and Mitchell, 1991). In sharp contrast to these high nutrient, low productivity oceanic habitats, regions exposed to the annual advance and retreat of sea ice, support seasonal phytoplankton blooms with high rates of primary production (Holm-Hansen et al., 1989; Moore et al., 1999; Robinson et al., 1999; Smith et al., 1996, 2001; Smith and Nelson, 1985). The Antarctic marine habitat experiences extreme seasonal cycles. The spring and summer seasons are characterized by increased solar radiation, in-

* Corresponding author. Tel.: +1-805-893-4709; fax: +1-805-893-2578.
E-mail address: ray@icess.ucsb.edu (R.C. Smith).

0304-4203/$ - see front matter © 2003 Elsevier B.V. All rights reserved.
doi:10.1016/j.marchem.2003.07.004

creasing temperatures and sea ice ablation all contributing to a decrease in mixed-layer depth. The fall and winter seasons are characterized by decreased solar radiation, decreasing temperature and sea ice formation which all contribute to deeper mixed-layer depths.

The capacity of the world's ocean to sequester CO_2 is dependent on the response of the biological and solubility pumps in altering CO_2 concentrations in the surface waters (Volk and Hoffert, 1985). The Southern Ocean's role in moderating increasing atmospheric CO_2 levels is uncertain because of unpredictable spatial and temporal heterogeneity of the biological and solubility pumps and the previously mentioned undersampling in critical regions. Although the flux of CO_2 into the Southern Ocean is predicted to be high, there is little long-term storage of CO_2 (Calderia and Philip, 2000; Sabine et al., 1999). Predicting future concentrations and estimating fluxes in data-poor regions requires accurate, predictive ecosystem models and an understanding of the processes controlling CO_2 variations temporally and spatially (Carrillo, 2002).

Measurements of atmospheric O_2/N_2 ratios may help constrain the contribution of biological processes to the oceanic uptake of atmospheric CO_2 (Bender et al., 1996; Keeling and Shertz, 1992; Sherr and Sherr, 1996). Seasonal changes in the O_2/N_2 ratio in air result from variations in net terrestrial and oceanic primary production and oceanic heating and cooling. In the Southern Hemisphere (especially the Southern Ocean), models predict marine autotrophic production and heterotrophic respiration control seasonal variations of the O_2/N_2 ratio in air (Keeling et al., 1993; Sherr and Sherr, 1996). Coupling atmospheric changes of O_2/N_2 ratios to oceanic biological production and consumption will require an understanding of the links between organic and inorganic carbon cycling in the ocean to O_2 fluxes at the air–sea interface. Additionally, the interaction between the physical, chemical and biological controls on O_2 and CO_2 concentrations must be understood to predict future changes of the ecosystem to climate change.

The marine environment west of the Antarctic Peninsula is situated in a climatically sensitive region that is an ideal location to investigate the interactions between biological, chemical and physical processes (Smith et al., 1999b). The environment includes an interseasonal and interannual variable ice zone, open ocean areas, shelf water and coastal regions. The Palmer Long-Term Ecological Research (Pal-LTER) Program was established in 1990 to study the physical determinants on the Antarctic marine ecosystem, especially the interconnections between climate variability and habitat variability, and response of the marine ecosystem to change. The central tenet of the Pal-LTER program is that the annual advance and retreat of sea ice is a major physical determinant of spatial and temporal changes in the structure and function of the Antarctic marine ecosystem, from annual primary production to breeding successes of krill and seabirds (Ross et al., 2000; Smith et al., 1995). The timing of the bloom in the region west of the Antarctic Peninsula may depend on a variety of interconnected factors including water column stability induced from seasonal sea-ice melt, light, temperature and nutrients (Smith et al., 1996). Even though phytoplankton blooms are transient events that follow the ice edge in open waters, the impacts on the annual fluxes of CO_2 have yet to be determined.

The use of ship-based underway systems has become prevalent in studies to map and understand CO_2 dynamics in open ocean and near shore areas (Sabine and Key, 1998; van Geen et al., 2000). Interpretation of data are often difficult because CO_2 variability is a function of the spatiotemporal scales of the controlling processe(s) (Simpson, 1985). Often, more than one process is responsible for controlling CO_2 concentrations. Simultaneous measurements of dissolved O_2 concentrations can help identify the processes that control seawater CO_2 (Alvarez et al., 2002; Bender et al., 2000; DeGrandpre et al., 1997, 1998; Robinson et al., 1999). For instance, a simultaneous detection of fCO_2 undersaturation and O_2 supersaturation, both with respect to the atmosphere would imply photosynthesis as a controlling process. Additionally, a source of simultaneous fCO_2 supersaturation and O_2 undersaturation is net respiration. The use of property-property relationships between $fCO_{2\{Sat\}}$, $O_{2\{Sat\}}$, temperature, salinity and chlorophyll *a* can help elucidate the relative role of physical, chemical and biological controls on CO_2 distributions.

The goal of this research was to determine the spatial and temporal O_2 and CO_2 distributions and the major processes regulating their concentrations in

Southern Ocean surface waters west of the Antarctic Peninsula. The ratio of $O_{2\{Sat\}}$ to $fCO_{2\{Sat\}}$ was used to elucidate processes controlling fCO_2 and O_2 distributions. Specific examples were taken from smaller subsets of the underway data to quantify changes in fCO_2 and O_2 partial pressures and concentrations.

2. Materials and methods

2.1. Setting

The Pal-LTER program was established in 1990 and conducts annual oceanographic research cruises over a geographically defined grid west of the Antarctic Peninsula (Waters and Smith, 1992). The entire Pal-LTER study region covers an area 900×200 km (Fig. 1). The grid consists of ten transect lines 100 km apart, roughly perpendicular to the coast, extending 200 km off-shore. The "grid lines" were labeled relative to the distance from the first line located just south of Marguerite Bay (i.e. 000.xxx to 900.xxx). Along each transect line, station locations were 20 km apart from nearshore to 200 km offshore (xxx.000 to xxx.200). Therefore, the station 300.200 would be located along the 300 line and approximately 200 km offshore. A smaller grid, located in Arthur Harbor was also sampled approximately three to four times throughout each cruise. Stations were also occupied within selected coastal areas such as Marguerite Bay and Crystal Sound (Fig. 1). Portions of this grid were sampled at least once per year in the months of January and February during the annual Pal-LTER cruise.

Data presented in this paper were obtained during the 1997 austral summer field season, when the 200–600 lines were sampled (Fig. 1). Data were also collected in the austral winter, July 1999, during a cruise to specifically study the formation of sea ice. During the winter cruise, only the 200 and 600 lines were sampled. These lines were located just off Marguerite Bay and Anvers Island.

2.2. Continuous underway sampling system

During the 1997 austral summer Pal-LTER field season (January 11–February 13) and winter ice processes study cruise (June 15 to 11 July 1999), an automated underway fCO_2, pH and O_2 measurement system was deployed on the *R/V Polar Duke* and *RVIB Nathaniel B. Palmer*. The underway system acquired seawater from the ship's bow intake located approximately 5 m below the sea surface, and atmospheric air collected from the top of the ship's bridge approximately 10–12 m above the sea surface. Surface seawater fCO_2 was determined by continuously pumping water through a counter flow rotating disk type equilibrator (Bjork, 1948; Cross et al., 1956; Sabine and Key, 1998; Schink et al., 1970) as described previously by Carrillo and Karl (1999). The mole fractions of CO_2 and water vapor were measured with a LICOR model 6262 infrared CO_2 and H_2O analyzer. The CO_2 mole fraction was converted to fCO_2 using the total pressure and the viral equations of state for CO_2 (DOE, 1994). The fugacity of $CO_{2\{Sat\}}$ was calculated using the equation:

$$fCO_{2\{Sat\}} = (\text{Measured } fCO_2 / \text{Atmospheric } CO_2) * 100$$

where atmospheric fCO_2 was 358 μatm. The continuous measurement system was periodically calibrated (every 2.5 h) with compressed gas standards with nominal mixing ratios of 259.28, 303.86 and 373.19 parts per million (ppm) by volume. These gas standards were calibrated with World Meteorological Organization (WMO) primary standards obtained and certified by the NOAA Climate Monitoring and Diagnostics Laboratory (CMDL). Equilibrator temperature was measured with an Omega RTD and system pressure was measured with a Setra pressure transducer. Between calibrations, equilibrator and atmospheric samples were measured every 5 min. The entire measurement system was automated using a PC computer and LabVIEW® software. Temperature and salinity were measured with a Sea-Bird thermosalinograph positioned at the intake which was periodically calibrated by bottle salinity.

Oxygen concentration was monitored with three Endeco type 1125 pulsed oxygen electrodes. Electrode output was calibrated daily to bottle oxygen samples taken from conductivity–temperature–depth (CTD) casts and with water collected from the

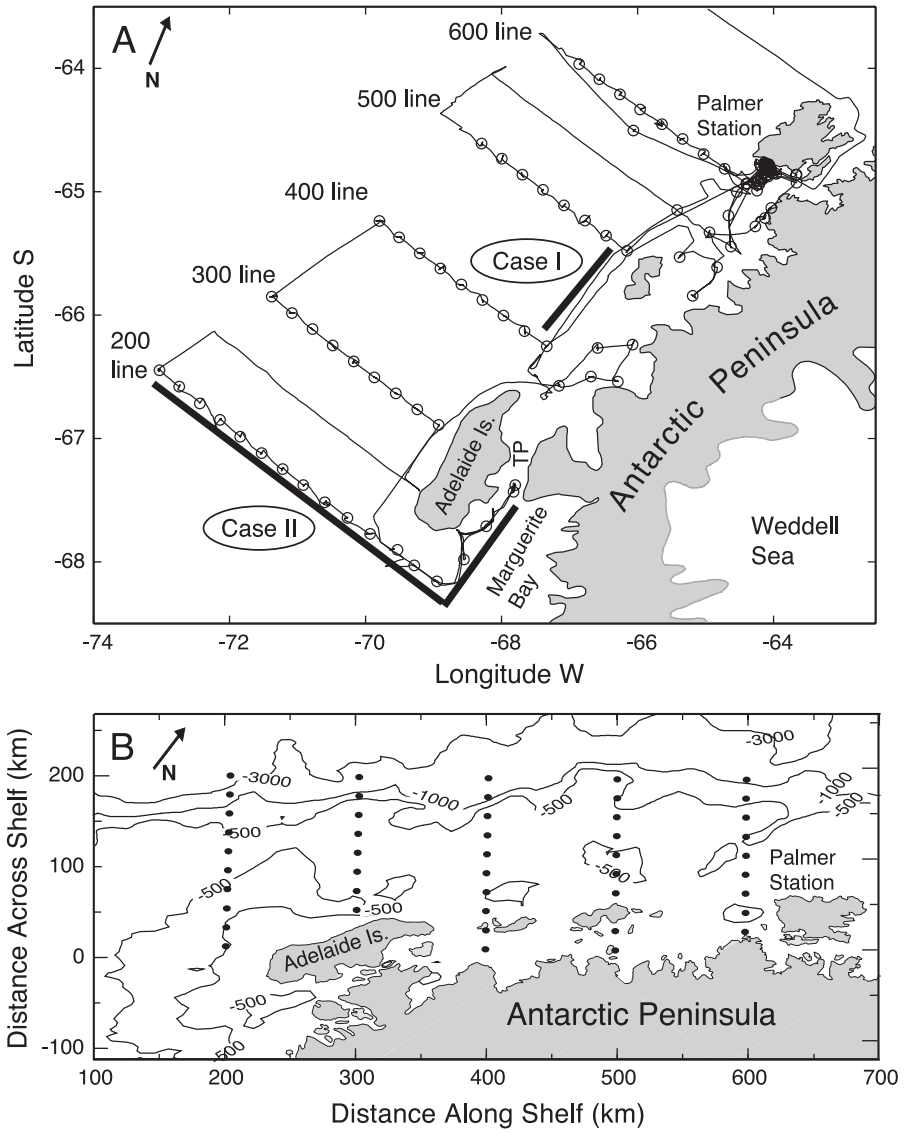


Fig. 1. (A) Long Term Ecological Research (LTER) program study area in the region west of the Antarctic Peninsula. Station locations are represented with open circles and the cruise track is represented by a solid line. Stations are located approximately 20 km apart perpendicular to the Peninsula and aligned in transects 100 km apart, parallel to the Peninsula. Tickle passage is represented with a TP. (B) Map of the LTER study area showing the bathymetric contours. Stations are represented by solid circles.

underway system just downstream from the electrodes. The overall mean and standard deviation between electrodes after calibration with discrete samples was 4.8 ± 5.4 μM ($n = 8198$). Oxygen saturation was calculated using the equations of Weiss (1970).

2.3. Net community production and dark community respiration

Net community production (NCP) and dark community respiration (DCR) were estimated by variations in O_2 and CO_2 during 24-h incubations in on-

deck incubators. The incubators were attached to the underway surface seawater system so samples were at surface seawater temperatures of −1.8 to 2.8 °C depending on location. Light experiments were exposed to daily incident radiance and dark experiments were incubated concurrently in solid plastic opaque coolers. All rates are presented as mmol m^{-3} day^{-1}. Typically, duplicate samples were taken at time 0 and time final (24 h), but at three stations, time course experiments (6-h intervals for 2 days) were conducted to test for linearity in the respiration rate. Dark incubation time-course data were fitted with a model I regression and displayed r^2 values greater than 0.95.

Water for oxygen incubation experiments was subsampled from CTD mounted 10-l Niskins into calibrated, approximately 140-ml dissolved oxygen sample bottles (iodine flasks). Samples were overflowed with 3 volumes and time zero samples fixed immediately. The remaining samples were capped with ground glass stoppers, sealed with polyethene tape and taken immediately to the incubators. After the appropriate incubation period (6, 12, 18, 24, 30, 48 h), samples were fixed and titrated within 24 h. The whole flask was titrated potentiometrically with a standardized solution (CSK standard) of sodium thiosulfate (HOT Program Protocols; http://www.hahana.soest.hawaii.edu/hot/protocols/protocols.html).

Changes in CO_2 were determined by direct measurements of dissolved inorganic carbon (DIC) following either light or dark incubations. Water was sampled in 300 ml Pyrex bottles similar to the oxygen samples and fixed by the addition of $HgCl_2$. Dissolved inorganic carbon was determined coulometrically using a Single Operator Metabolic Multi-parameter Analyzer (SOMMA) system in the laboratory at the University of Hawaii (Johnson et al., 1987). Oxygen and DIC measurements had analytical precisions of approximately 0.05% over the concentration ranges observed in this study.

2.4. Ancillary data

Water samples were obtained from discrete water depths at hydrographic stations using a Bio-optical Profiling System (BOPS; Smith et al., 1984). This system includes a Sea Bird CTD mounted on a rosette with Go Flo bottles. Chlorophyll *a* samples were collected during the cruise from the underway surface seawater system and from the BOPS. Chlorophyll *a* was extracted and analyzed using fluorometer standard methodology (Smith et al., 1981). Samples were collected for nutrients (nitrate + nitrite) and analyzed using a Technicon Autoanalyzer.

3. Results

3.1. Data overview

Analysis of the underway system data showed surface seawater fCO_2 pressure in 1997 ranged from 100 to 390 μatm compared to a mean atmospheric value of 358 ± 3 μatm for the Pal-LTER region (Fig. 2A). Surface seawater O_2 concentrations ranged from 300 to 550 mmol m^{-3} (Fig. 2B). Temperature ranged from −1.8 to 2.7 °C and salinity ranged from 29.5 to 33.8 (Fig. 2C and D). All parameters showed a high degree of variability especially occurring on or after year day 35. This period corresponds to a time during transit into Marguerite Bay and the northbound transit near the coast.

Plots of $fCO_{2\{Sat\}}$ versus salinity and temperature showed little correlation (Fig. 3A and B). However, $fCO_{2\{Sat\}}$ and $O_{2\{Sat\}}$ showed a much better coherence (Fig. 3C). Typically, areas of surface ocean fCO_2 supersaturation were found at the outer shelf and areas of undersaturation were encountered in coastal waters, so $fCO_{2\{Sat\}}$ typically increased with increasing distance from shore (Fig. 4A). Generally, colder fresher waters were encountered near the coast and warmer saltier waters were found off-shelf (Fig. 4B and C).

These underway data segregated into one of four quadrants on a graph of $O_{2\{Sat\}}$ versus $fCO_{2\{Sat\}}$, with the origin at 100% $O_{2\{Sat\}}$ and 100% $fCO_{2\{Sat\}}$ (Fig. 3C). Plotting the spatial distribution of points based on their quadrant location from Fig. 3C showed that most points in quadrant I were located in Marguerite Bay and near the coast (Fig. 4D). The maximum $O_{2\{Sat\}}$ (155%, 550 mmol m^{-3}) and minimum $fCO_{2\{Sat\}}$ (35%, 90 μatm) were found in Marguerite Bay. Generally, data in quadrant II were found in the southern offshore region of the Pal-LTER grid between the 200 and 400 line (Fig. 3D and 4D). These values represent slight O_2 and fCO_2 supersaturations and were correlated with the warmest (2.5 °C) surface waters encountered (Fig. 4B).

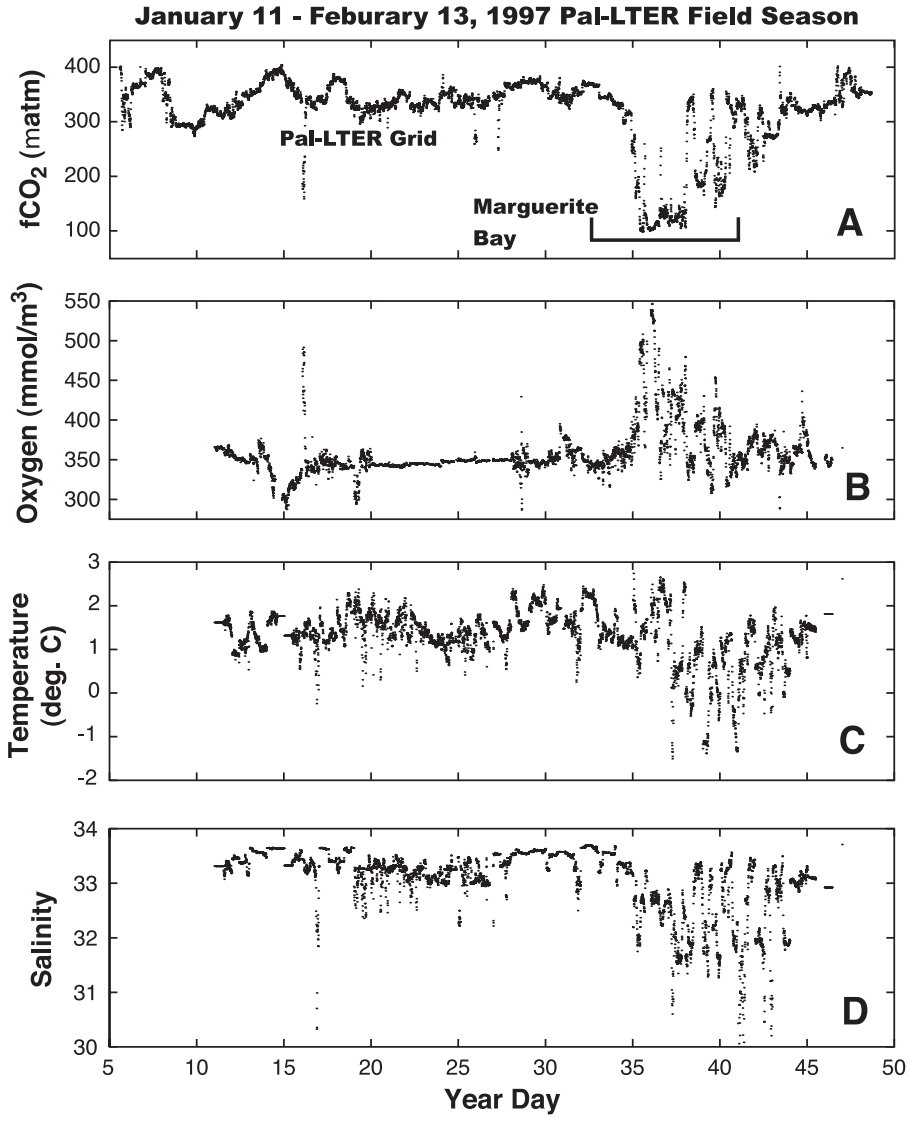


Fig. 2. Year day (1997) versus (A) fCO_2 (μatm), (B) oxygen concentration (mmol m^{-3}), (C) temperature (°C) and (D) salinity.

Data in quadrant III were located in the northern offshore region between the 500 and 600 line. These values were slightly supersaturated with respect to fCO_2 and undersaturated with respect to O_2. Data collected during the austral winter, July 1999, are represented by a filled circle located in quadrant III with the standard deviations represented by the vertical and horizontal lines. Winter data show an undersaturation of O_2 (92%) and supersaturation of fCO_2 (110%). Finally, data in quadrant IV were located generally near the coast. These values represent fCO_2 and O_2 undersaturation states. Two case studies are presented to illustrate the time and space variability of CO_2 and O_2 inventories.

3.2. Case study I: effect of cooling and net organic matter production

Effects of cooling and net organic matter production on $O_{2\{Sat\}}$ and $fCO_{2\{Sat\}}$ can be illustrated using a

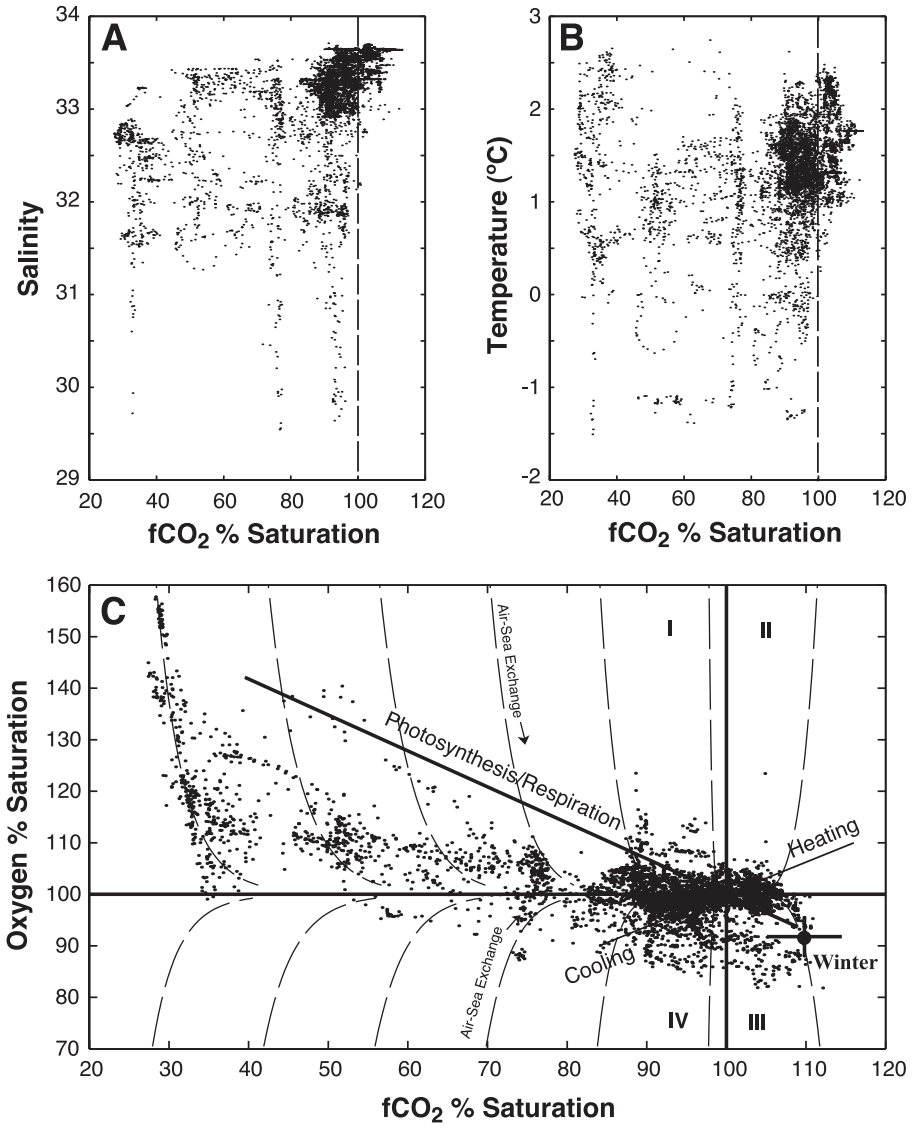


Fig. 3. The fugacity of CO_2 versus (A) salinity and (B) temperature. The vertical dashed lines represent 100% $fCO_{2\{Sat\}}$. (C) The fugacity of CO_2 % versus O_2 %saturation. Vertical and horizontal solid lines represent 100% saturation levels of O_2 and fCO_2. The intersection of these lines in the lower right corner denotes the origin and represents 100% O_2 and fCO_2 air-saturation. Based on these lines, the figure is separated into four quadrants. Quadrant I is located in the upper left corner. Quadrant II is located in the upper right corner. Quadrant III is located in the lower right corner. Quadrant IV is located in the lower left corner. The filled circle in quadrant III represents the mean of data collected during the austral winter, July 1999. The standard deviations are represented by the horizontal and vertical lines. The solid line that extends from the origin into quadrant I represents production of O_2 and consumption of CO_2 at a theoretical $PQ_{[Sat]}$ of -0.7. The solid line that extends from the origin into quadrant II represents heating with a temperature change of $+4.0$ °C. The dashed line that extends from the origin into quadrant IV represents cooling with a temperature change of -4.0 °C. Dashed lines represent the $O_{2\{Sat\}}/fCO_{2\{Sat\}}$ values based on a model of air to sea exchange.

subset of the underway data. On Jan. 27, a 159-km transect was conducted parallel to the Antarctic Peninsula approximately 50 km offshore between 67.5° and 65.5°W (400–550 line; Fig. 1A). Approximately 2 weeks later (Feb. 9–10), this area was resampled from south to north. The initial survey on Jan. 27

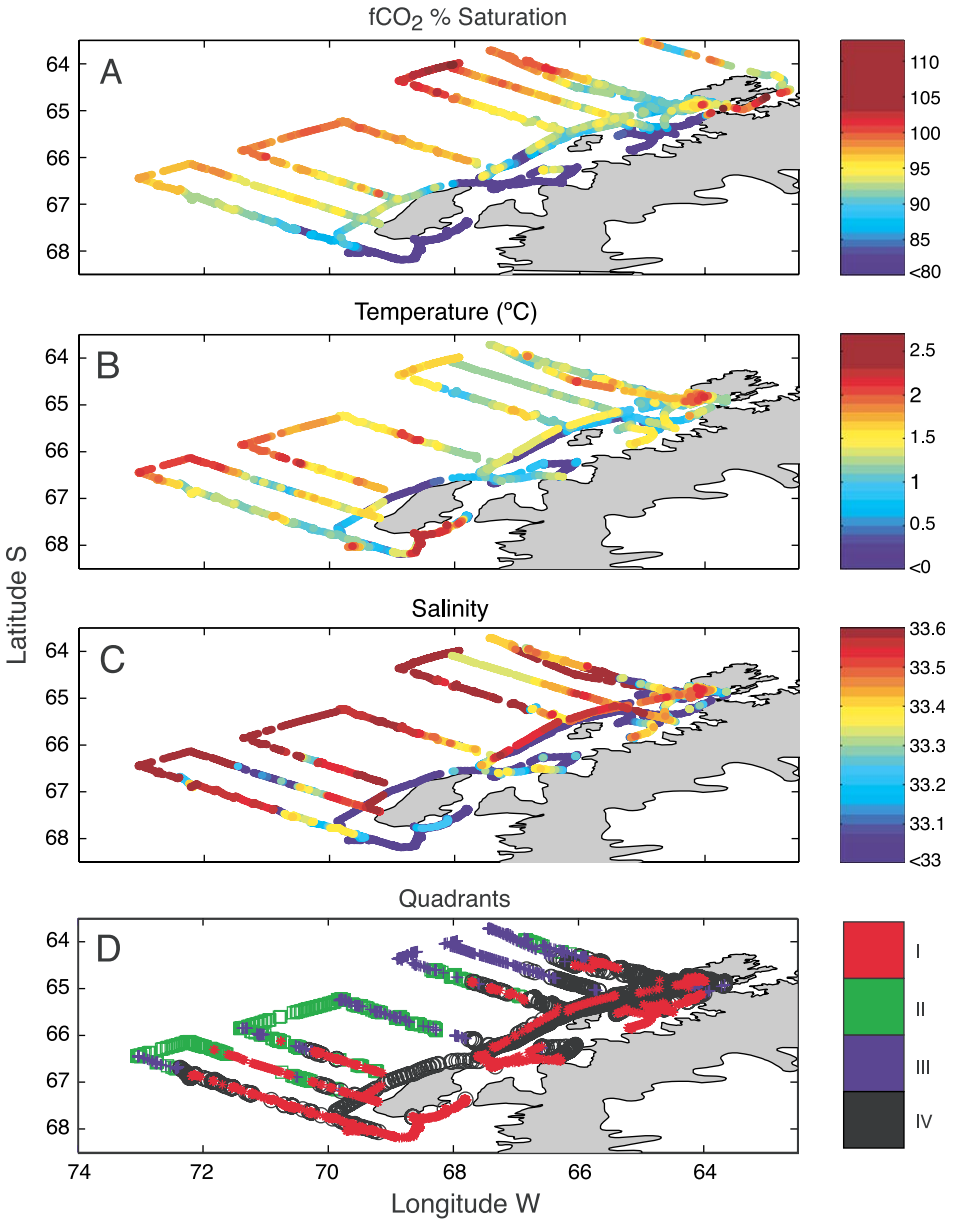


Fig. 4. Spatial distribution of (A) fCO_2 saturation, (B) temperature, (C) salinity and (D) quadrant position as defined in Fig. 3C.

showed temperature, salinity and $O_{2\{Sat\}}$ were relatively constant at 1.5 ± 0.1 °C, 33.5 ± 0.1% and 100.0%, respectively (Fig. 5A–C). The fugacity of CO_2 was nearly constant at 97.0 ± 1.1% with the exception of an anomalously low spike (70% saturation) at approximately 67.0°W (Fig. 5D). Chlorophyll *a* concentrations at stations 400.040 and 500.040 during the Jan. 27 transect were 0.6 mg m^{-3} (Fig. 5E).

On Feb. 9–10, during the second survey of this area, temperature and salinity showed an overall cooling and a freshening. In the southern portion of the transect, temperature ranged from 0 to −1.5 °C and salinity

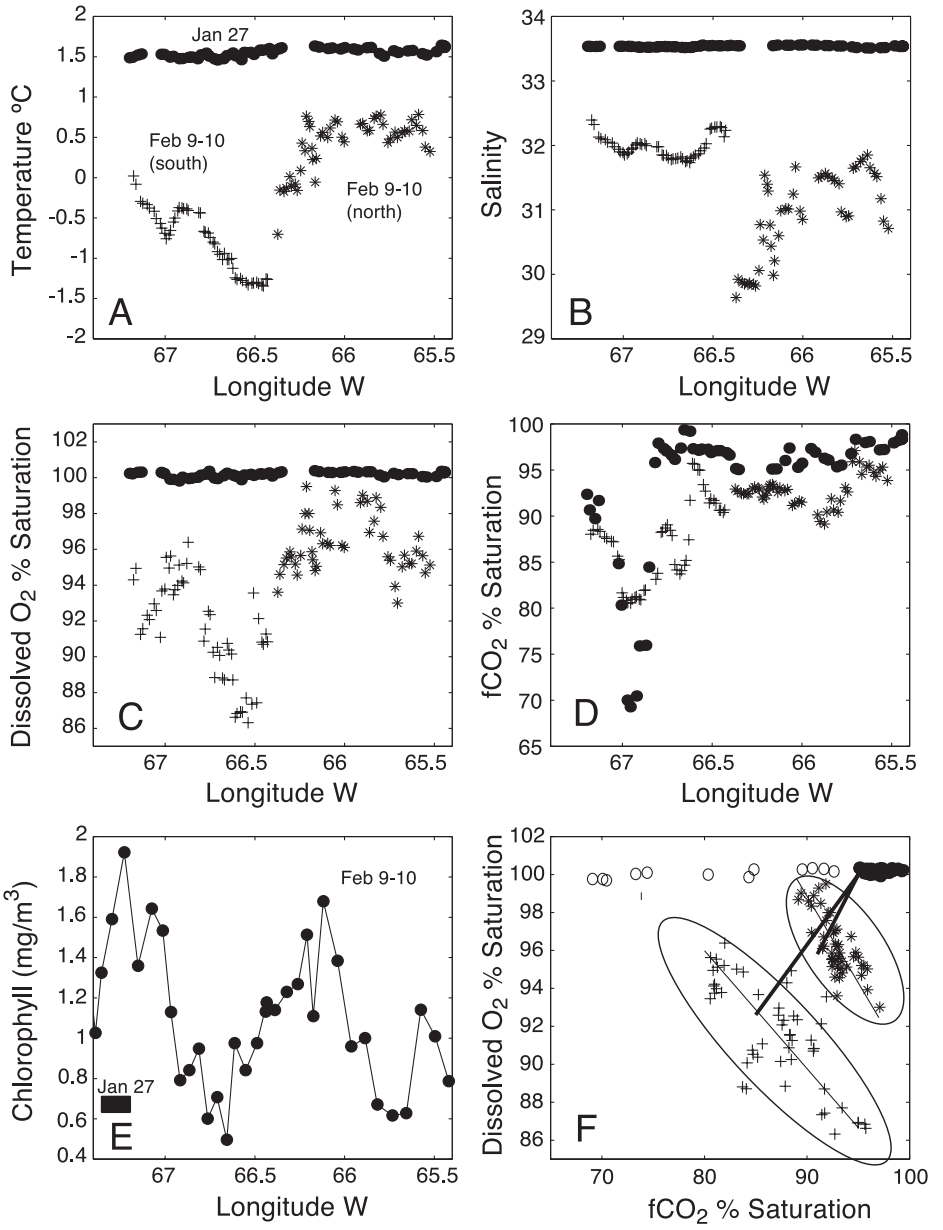


Fig. 5. Longitude W versus (A) temperature, (B) salinity, (C) O_2 saturation, (D) fCO_2 saturation and (E) chlorophyll (mg/m^3). (F) The fugacity of CO_2 saturation versus O_2 saturation. Filled circles represent values from the Jan. 27 transect. Plus signs represent values from the southern half of the Feb. 9–10 transect. Asterisks represent values from the northern half of the Feb. 9–10 transect. The two thick lines show the predicted values of fCO_2 and O_2 based on a cooling of -2.5 and -1 °C and freshening of 1.5 and 2.5 as described by the changes in temperature and salinity between transects (Weiss, 1970). The two thin lines within the ellipses were fit using a model II linear regression (geometric mean) for the northern and southern cluster of points representing the Feb. 9–10 data with slopes of -0.6 (-0.5 to -0.8 at the 95% confidence interval) and -0.9 (-0.7 to -1.2 at the 95% confidence interval), respectively.

ranged from 31.9 to 32.1 (Fig. 5A and B). In the northern portion of the transect, temperatures ranged from 0 to 0.5 °C and salinity ranged from 29.5 to 31.5. Oxygen saturation decreased overall with values ranging from 86% to 95% in the southern portion of the transect to 95% to 99% in the north (Fig. 5C).

The fugacity of CO_2 generally showed a decrease in saturation except for the area that had a relatively low fCO_2 value on Jan. 27 (Fig. 5D). In the northern portion of the transect, values ranged from 90% to 97% saturation. In the south, values ranged from 80% to 96% saturation. Chlorophyll samples were taken from the underway system during the transect north (Feb. 9–10) and values ranged from a maximum of 1.9 to a minimum of 0.5 mg m^{-3} (Fig. 5E).

A graph of $O_{2\{Sat\}}$ versus $fCO_{2\{Sat\}}$ was described by three clusters (Fig. 5F). A positive correlation was shown between the cluster representing Jan. 27 data (in the upper right hand corner) and clusters representing the north and south components the Feb. 9–10 data (shown to the lower left). The data shown by the 12 open circles were not used in the correlation analysis and represent the low $fCO_{2\{Sat\}}$ spike (Fig. 5F). Fitted lines show the predicted values of fCO_2 and O_2 based

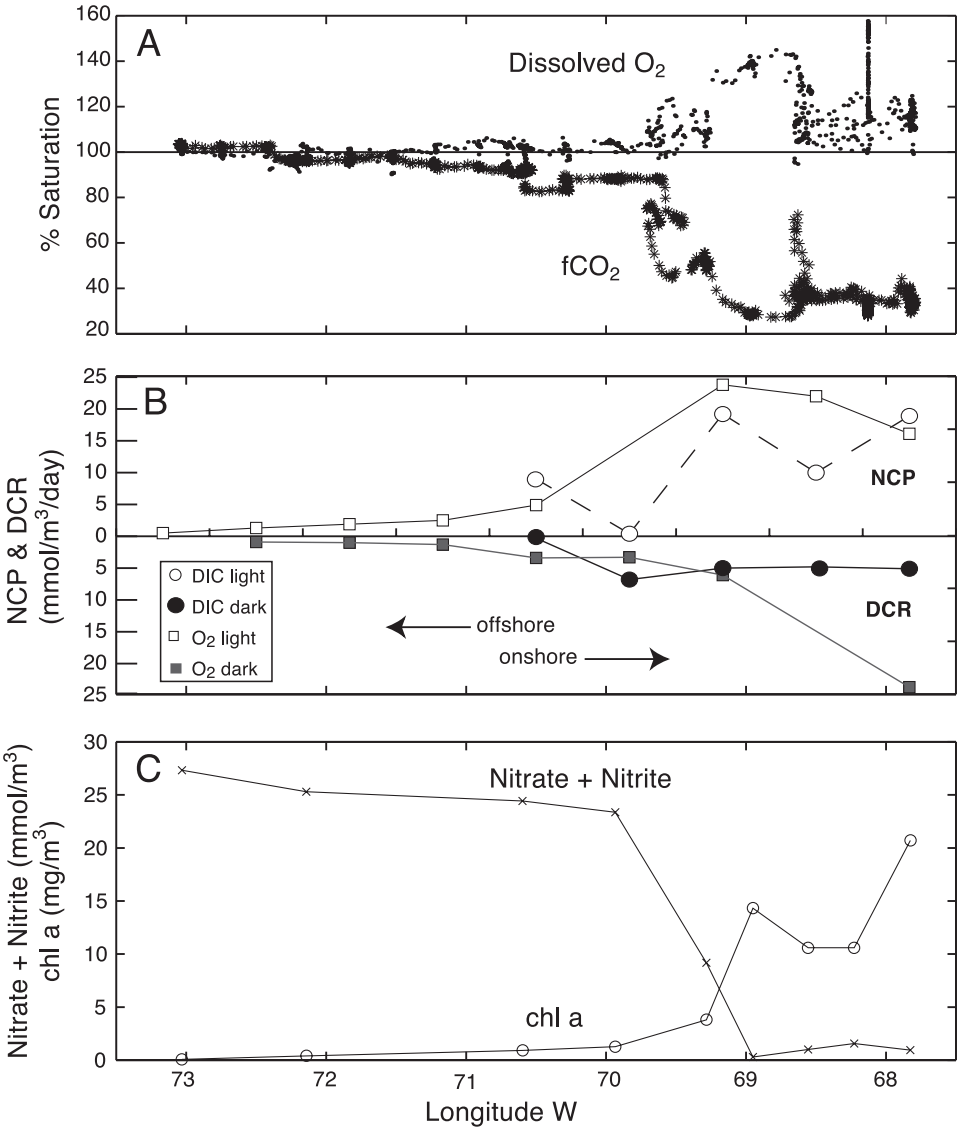


Fig. 6. Longitude versus (A) fCO_2 and O_2 saturation. (B) Net community production and dark community respiration measured by DIC and O_2 light dark bottle incubations (C) [nitrate + nitrite] and chlorophyll *a* concentrations.

on a cooling of −2.5 and −1 °C and freshening of 1.5 and 2.5 as described by the changes in temperature and salinity between transects (Fig. 5A and B; Weiss, 1970). A model II linear regression (geometric mean) was fit for the northern and southern cluster of points representing the Feb. 9–10 data with slopes of −0.6 (−0.5 to −0.8 at the 95% confidence interval) and −0.9 (−0.7 to −1.2 at the 95% confidence interval), respectively.

3.3. Case study II organic matter production, respiration and air-to-sea exchange

A second case study illustrates the effect of net organic matter production, respiration and air–sea exchange in determining the $O_{2\{Sat\}}/fCO_{2\{Sat\}}$ of surface waters. Between Feb. 1 and 3, a 300-km offshore to onshore transect was conducted into Marguerite Bay. Oxygen saturation increased off to onshore into Marguerite Bay with values ranging from 95% to 158% (Fig. 6A). In contrast, the fugacity of $CO_{2\{Sat\}}$ decreased from offshore to onshore with values ranging from 105% to 27% (Fig. 6A). Salinity decreased offshore to onshore with values ranging from 33.6 to 30.5 (Fig. 4C). Temperature generally decreased from offshore to onshore (with values ranging from 2.5 to 0.5 °C), except within Marguerite Bay where temperatures were relatively warm at 1.7 °C (Fig. 4B).

NCP increased from offshore to onshore with the exception of one station in Marguerite Bay. Estimates based on changes of oxygen in light bottles ranged from −0.9 to 23.8 mmol O_2 m^{-3} day^{-1} (Table 1, Fig. 6B). Within Marguerite Bay estimates of NCP based on changes of DIC in light bottles range from 0.4 to 19.2 mmol C m^{-3} day^{-1}. DCR also increased from off to onshore. Estimates of DCR based on changes of O_2 in dark bottles ranged from 0.9 to 23.7 mmol O_2 m^{-3} day^{-1} (Fig. 6B). Within Marguerite Bay estimates of DCR based on changes of DIC in dark bottles ranged from 0.3 to 6.8 mmol C m^{-3} day^{-1}. Chlorophyll *a* concentrations increased offshore to onshore with values ranging from 0.1 to 20.7 mg m^{-3} (Table 1, Fig. 6C). Nitrate plus nitrite concentrations decreased from offshore to onshore with concentrations ranging from 0.3 to 27.3 mmol m^{-3} (Table 1, Fig. 6C).

4. Discussion

4.1. Background

The variability shown by the underway measurements (Fig. 2) reflects a combination of processes controlling O_2 and fCO_2, including net community production, dark community respiration, temperature-driven solubility changes and air–sea gas fluxes (Table 2). Except for air–sea gas exchange, all of

Table 1
Net community production and dark community respiration estimated by the oxygen and dissolved inorganic carbon light/dark bottle incubation method

Station	DIC (mmol m^{-3} day^{-1}) (0.7 ± 0.7, $n=7$)[a]				O_2 (mmol m^{-3} day^{-1}) (0.6 ± 0.5, $n=21$)[a]							
	Gross	NCP	DCR	P/R	Gross	NCP	DCR	P/R	PQ	RQ	NO_3+NO_2 (μM)	Chl *a* (mg m^{-3})
200.200	***	***	***	***	***	0.5	***	***	***	***	27.3	0.1
200.140	***	***	***	***	2.2	1.3	0.9	2.4	***	***	25.3	0.4
200.040	***	***	***	***	2.9	1.9	1.0	2.9	***	***	24.4	0.9
200.000	***	***	***	***	3.8	2.5	1.3	o.6	***	***	23.4	1.3
200.-040	9.3	9.0	0.3	31.0	8.3	4.9	3.4	2.4	0.9	0.1	9.2	3.8
200.-060	7.2	0.4	6.8	1.1	2.3	−0.9	3.3	0.7	0.3	2.1	0.3	14.3
mb1[b]	24.2	19.2	5.0	4.8	30.0	23.8	6.1	4.9	1.2	0.8	1.0	10.6
mb2	14.8	10.0	4.8	3.1	19.9	22.0	***	***	1.3	***	1.6	10.6
tp[c]	24.0	18.9	5.1	4.7	39.8	16.1	23.7	1.7	1.7	0.2	0.9	20.7

*** No data.
[a] Mean difference between replicate samples.
[b] Marguerite Bay.
[c] Tickle passage.

Table 2
Summary of processes affecting upper ocean O_2 and fCO_2

Process	O_2 % saturation	fCO_2 % saturation
Increase temp.	+2.5%/°C	+4%/°C
Decrease temp.	−2.5%/°C	−4%/°C
Production	+1% $O_{2\{Sat\}}$/2% $fCO_{2\{Sat\}}$	−1% $O_{2\{Sat\}}$/2% $fCO_{2\{Sat\}}$
Respiration	−1% $O_{2\{Sat\}}$/2% $fCO_{2\{Sat\}}$	+1% $O_{2\{Sat\}}$/2% $fCO_{2\{Sat\}}$

these processes drive O_2 and fCO_2 away from air-saturated equilibrium values at fairly well constrained stoichiometric proportions (Table 2). However, air–sea gas exchange will drive saturation back to atmospheric equilibrium concentrations at stoichiometric proportions that are dependent on the air–sea O_2 and fCO_2 gas flux.

Oxygen and fCO_2 saturation are affected by temperature and salinity. An increase in temperature produces an increase in both the O_2 and fCO_2 saturation state and a decrease in temperature produces a decrease in both the O_2 and fCO_2 saturation state. Salinity has less of an effect than temperature. The range of salinity encountered over the cruise produces only a 2.5% range in $O_{2\{Sat\}}$ while the range of observed temperatures produces a 11.2% range in $O_{2\{Sat\}}$. The $\Delta fCO_{2\{Sat\}}/\Delta O_{2\{Sat\}}$ ratio for heating and cooling is 1.7 (Fig. 3C). Biological oxygen production is coupled to biological organic carbon production through the photosynthetic quotient (i.e. PQ). The gross photosynthetic quotient is the molar ratio of oxygen production to the rate of inorganic carbon utilization; PQ values are generally in the range of 1.3 ± 0.1 depending upon the source of N (NH_4^+ versus NO_3^-; Laws, 1991). Using a Revelle factor of 14, a 1 mmol m^{-3} change in DIC is equivalent to a 1.9 μatm change in fCO_2 (Takahashi et al., 1980a). Assuming a atmospheric fCO_2 value of 350 μatm and a O_2 saturation concentration of 350 mmol m^{-3}, PQ = 1.3 = 1.3 mmol O_2 m^{-3}/1 mmol DIC m^{-3} = 1.3 mmol O_2 m^{-3}/1.9 μatm fCO_2 = 0.0037 O_2 %Sat/0.0054 fCO_2 %Sat = 0.7. If the PQ is expressed in terms of O_2 and fCO_2 saturation states, $PQ_{[Sat]}$ is 0.7 (i.e. $\Delta O_{2\{Sat\}}/\Delta fCO_{2\{Sat\}} = PQ_{[Sat]} = 0.7$).

Air–sea exchange rates differ for O_2 and fCO_2. Timescales range from days to weeks for O_2 and months for fCO_2 (Appendix A; Broecker and Peng, 1982). In surface seawater, the disequilibrium between the partial pressure of a gas in the overlying atmosphere and that in surface water drives a bi-directional flux across the air–sea interface in the direction towards equilibrium (Kanwisher, 1963). The net flux is a function of the gas transfer coefficient (also referred to as the piston velocity coefficient), solubility and difference in gas partial pressure. The gas transfer coefficient is a function of gas diffusion and stagnant film thickness but is usually parameterized by wind speed (Liss and Merlivat, 1986; Smith, 1985; Wanninkhof, 1992).

4.2. Spatial and seasonal variations of gas saturation states

Oxygen and fCO_2 varied significantly from air-saturated equilibrium states suggesting a combination of processes controlling O_2 and fCO_2 distributions within the Pal-LTER study region (Fig. 2). The correlation of $O_{2\{Sat\}}$ to $fCO_{2\{Sat\}}$ as indices of chemical, physical and biological processes on variable time scales has not been used extensively but could be a useful parameter for studying ecosystem dynamics. For example, in the Pal-LTER study region, the maximum $fCO_{2\{Sat\}}$ of 112% coincided with the minimum $O_{2\{Sat\}}$ 81% and the maximum $O_{2\{Sat\}}$ of 157% coincided with the minimum $fCO_{2\{Sat\}}$ of 27%. A possible source of simultaneous fCO_2 undersaturation and O_2 supersaturation was photosynthesis, and the possible mechanism leading to simultaneous fCO_2 supersaturation and O_2 undersaturation was net respiration. Consequently, over relevant time and space scales, the correlation between $O_{2\{Sat\}}$ and $fCO_{2\{Sat\}}$ could help constrain the net autotrophic/heterotrophic ecosystem balance.

Overall, the most significant correlation observed was the negative one between $O_{2\{Sat\}}$ and $fCO_{2\{Sat\}}$ (Fig. 3C). The model II linear regression (geometric mean) slope was −0.4, which was about 40% less than the theoretically calculated slope of −0.7 describing net organic matter production. This was most likely a result of the competing processes of organic matter production and differential air–sea gas exchange affecting the O_2/fCO_2 ratios. As photosynthesis produces O_2 and depletes CO_2 concentrations in surface seawater, air–sea gas exchange will ventilate the supersaturated O_2 more rapidly than it will replenish the undersaturated CO_2 (Appendix A). At high O_2 concentrations (>120% saturation),

the $O_{2\{Sat\}}/fCO_{2\{Sat\}}$ ratio for air–sea gas exchange was approximately 3. As O_2 concentrations approach atmospheric equilibrium, the ratio of $O_{2\{Sat\}}/fCO_{2\{Sat\}}$ decreases. The overall effect was a lowering of the slope of the $O_{2\{Sat\}}$ versus $fCO_{2\{Sat\}}$ regression.

Changes in fCO_2 concentrations cannot be explained by temperature variations alone. The range of temperatures encountered for the grid was approximately 4 °C. The solubility change calculated for a warming or cooling of 4 °C is approximately 48 μatm (Weiss, 1974). Therefore, temperature variations can only account for at most 20% of the full range of measured fCO_2 concentrations.

Klinck (1998) presented a physical description of the seasonal changes of heat and salt in the Pal-LTER study area. During the winter, surface waters are near freezing (−1.8 °C) and have a salinity range from 33.8 to 34.1. During the transition from fall to winter, surface seawaters are cooled by decreasing atmospheric temperatures and wind-driven heat exchange. As surface water densities increase, surface stratification decreases and waters are mixed with deeper waters of low O_2 and high CO_2. This was reflected by the relatively constant fCO_2 supersaturation and O_2 undersaturation observed during the winter (Fig. 3). The depth of the winter mixed-layer will determine the O_2 and CO_2 winter surface concentrations through changes in the mixed layer depth (Gordon and Huber, 1990; Smith et al., 1999a).

Between winter and summer, solar insolation increases and sea ice melts; air–sea exchange will drive gas pressure towards air-saturated equilibrium values. In localized areas, especially near the coast, melting glacial ice can cool and freshen surface waters which decrease O_2 and fCO_2 saturation states. As noted by Dierssen et al. (2002), glacial meltwater also enhances water column stability and subsequent phytoplankton growth. In areas of net organic matter production, positive net photosynthesis decreases fCO_2 and increases O_2 concentrations. Within ice-free areas, warming and freshening will increase O_2 and fCO_2 saturation states.

The spatial distribution of values clustered between 90% and 110% $fCO_{2\{Sat\}}$ and 85% to 110% $O_{2\{Sat\}}$ implied surface seawater within the Pal-LTER region remained close to atmospheric equilibrium during January. This cluster accounts for >80% of the total area surveyed in the Pal-LTER grid. The remaining $O_{2\{Sat\}}/fCO_{2\{Sat\}}$ values represented a large disequilibrium and were found in Marguerite Bay and isolated coastal areas. These areas represented a large biological signal but accounted for a smaller fraction of the area surveyed.

The spatial distribution of $O_{2\{sat\}}/fCO_{2\{Sat\}}$ values within the Pal-LTER grid was the result of a variety of competing ecosystem processes that affect fCO_2 and O_2. Quadrant I data depicted areas of fCO_2 undersaturation and O_2 supersaturation implying a biological source (net photosynthesis). These conditions were most often located in protected coastal waters where near surface stratification is typically enhanced by glacial or sea-ice melt (Dierssen et al., 2002).

Quadrant II data were representative of outer stations along the 200 line and correlate well with warmer (>2.5 °C) offshore waters. These local warm waters could be the result of localized heating since mixed layer depths were relatively shallow (10 m), but may also derive from the southern edge of the Antarctic circumpolar current (Hofmann et al., 1996).

Quadrant III data derive from the offshore stations along the 600 line where relatively cooler surface water temperatures prevail. In contrast to the offshore waters in the southern region, the off-shelf region to the north showed slight fCO_2 supersaturations and O_2 undersaturations (quadrant III; Fig. 3) that intrude onto the shelf. Surface water temperatures were somewhat cooler in the northern than in the southern region, with deeper mixed layer. One prominent deep channel (500 m) extends to the northwest of Anvers Island. These canyons can act as conduits for water to move onto the shelf as inferred from temperature and salinity changes over deeper areas of the shelf (Klinck, 1998). The northern region gas characteristics, fCO_2 supersaturation and O_2 undersaturation, implied upwelling as a potential source for the CO_2-enriched and O_2-depleted waters. Alternatively, in the southern region, we hypothesize that localized stratification and heating may be responsible for the fCO_2- and O_2-enriched waters.

Areas of fCO_2 undersaturation and O_2 undersaturation (quadrant IV) were generally encountered in coastal and on-shelf waters (Fig. 4D). Data within quadrant IV occur along the coast where glacial melt may continuously freshen and cool the surface waters through the summer months. The freshening and cooling drive local sinks for O_2 and fCO_2 throughout

the spring and summer seasons. Additionally, areas of ice melt are potential sites for phytoplankton bloom formations which can further increase fCO_2 undersaturations. Ecosystem processes resulting in the quadrants I and IV data are discussed more thoroughly in the following two case study sections.

4.3. Case study I: effects of cooling and net organic matter production

An unexpected result of our analysis of the underway system data were the positive correlation of $fCO_{2\{Sat\}}$ and $O_{2\{Sat\}}$ for a repeat transect separated by 14 days. This result was consistent with surface water cooling. The positive correlation of fCO_2 with temperature is generally found only in open ocean oligotrophic environments and is not expected for more eutrophic coastal environments where biological processes dominate (Carrillo, 2002; Takahashi et al., 1993). However, Antarctic coastal waters are a variable mosaic in both time and space due to patchy plankton blooms and the effect of glacial and sea-ice melt on surface waters close to the continent.

In the Pal-LTER study region, fresher waters were typically found close to the continent where glacial and sea ice meltwaters can affect the local heat and salt budgets compared to saltier waters found offshore (Dierssen et al., 2002; Klinck, 1998). Variations in temperature and salinity between transects were consistent with the advection and melting of ice (Ohshima et al., 1998). Ice is advected into an ice-free area that has been previously warmed by solar radiation. The advection of ice overwhelms the local balance of heat and salt causing both a decrease in temperature and salinity.

During the Jan. 27, southbound transit, temperature, salinity and $O_{2\{Sat\}}$ were spatially invariant suggesting a relatively homogenous water mass (Fig. 5A–C). The fugacity of $CO_{2\{Sat\}}$ was also spatially invariant except for an anomalous low spike in fCO_2 saturation at approximately 66°S and 67°W (Fig. 5D). Because the surface exposure history of this water mass was unknown, we can only speculate about the anomalous signal. It may be a remnant of an earlier bloom where carbon dioxide was removed but not yet replenished by gas exchange with the atmosphere or respiration.

The positive regression shown between cluster I, Jan. 27, southbound transit, and clusters II and III, Feb. 9–10 northbound transit imply cooling had lowered $O_{2\{Sat\}}$ and $fCO_{2\{Sat\}}$ (Fig. 5F). Predicted changes of O_2 and fCO_2 based on cooling and freshening trends matched observed values reasonably well (Table 3, Fig. 5F). A comparison of calculated and measured values showed differences no greater than 2% for either fCO_2 or O_2 saturation states.

Superimposed on the temporal physical signal was a spatially variable biological signal. Comparison of O_2 and fCO_2 saturation showed a positive correlation if the values were clustered according to the temperature and salinity characteristics. Surface waters located south were colder and saltier, relative to surface waters, in the north. Three scenarios may help to explain these T–S characteristics. First, a different water mass may have advected into the area with different temperature and salinity characteristics. Second, differential ice melting with more ice ablation in the northern than in the southern sector may have contributed to the different temperature and salinity characteristics. Third, differential mixing or upwelling of colder saltier waters in the southern section may have contributed to the different temperature and salinity characteristics. Unfortunately, we cannot distinguish among these possibilities and the T–S characteristics may be a combination of any of the three.

Table 3
Transect properties

Date	Temp.	Salinity	Chl *a*	$O_{2\{Sat\}}$ calc.[a]	$O_{2\{Sat\}}$ meas.	$fCO_{2\{Sat\}}$ calc.[b]	$fCO_{2\{Sat\}}$ meas.
Jan. 27	1.5 ± 0.1	33.5 ± 0.1	0.6	100.4	100.2 ± 0.1	95.0[c]	97.0 ± 1.1
Feb. 9–10 (southboundtransit)	-1.0 ± 0.3	32.0 ± 0.2	1.2	92.7	91.6 ± 2.8	85.3	87.1 ± 4.5
Feb. 9–10 (northboundtransit)	0.5 ± 0.2	31.0 ± 0.4	1.2	95.8	96.3 ± -1.6	91.1	92.8 ± 1.7

[a] Calculated dissolved O_2 saturation based on Weiss (1970).
[b] Calculated fCO_2 based on Goyet et al. (1993).
[c] Measured.

The negative regression between $O_{2\{Sat\}}$ and $fCO_{2\{Sat\}}$ in clusters II and III indicated that net community production and dark community respiration were first-order controlling factors. The negative correlation between $O_{2\{Sat\}}$ and $fCO_{2\{Sat\}}$ also correlated with a two-fold increase in chl *a* concentration, from 0.6 to 1.2 mg m^{-3}. Overall, this case study was an example where the physical process of cooling lowered O_2 and fCO_2 saturation in a coastal area. A spatial biological signal was then superimposed onto the temporally varying temperature signal. Quantification of both processes in space and in time is required to constrain CO_2 budgets in this area.

4.4. Case study II: organic matter production, respiration and air-to-sea exchange

Biological production of organic matter can have a significant effect on O_2 and CO_2 concentrations on small spatial scales (<10 km) and short time scales (<1 week; Carrillo and Karl, 1999; Holm-Hansen and Mitchell, 1991; Karl et al., 1991). The effect of biological production on the ambient $O_{2\{Sat\}}/fCO_{2\{Sat\}}$ was seen in the offshore to onshore transect into Marguerite Bay (Fig. 6A). Offshore waters were characteristic of high nutrient, low chlorophyll surface waters with low rates of NCP and DCR. Corresponding O_2 and fCO_2 saturation states were very close to equilibrium with the atmosphere, which also suggests very low biological activity and very little heating or cooling. Net community production increased with decreasing distance from shore. Nitrate, nitrite and fCO_2 saturation showed corresponding decrease suggesting the overall effect of NCP in controlling fCO_2 values. Areas of fCO_2 undersaturation (30%) and O_2 supersaturation (155%) were encountered in Marguerite Bay and were associated with accumulations of chlorophyll *a* indicating a biological source. Within Marguerite Bay, the effect of net organic matter production on O_2 and fCO_2 are clearly shown. Increased O_2 and chlorophyll *a* concentrations were correlated with a decreased $[NO_3+NO_2]$ and fCO_2. Marguerite Bay is near the head of a submarine canyon that may sustain large phytoplankton blooms by an enhanced macro and micro-nutrient supply via topographic routing of deep waters (Hofmann et al., 1996; Klinck, 1998). These biological hotspots may also facilitate carbon and energy transfer to the higher trophic levels.

The effect of respiration on O_2 and CO_2 was less obvious. The importance of heterotrophic microbes (bacteria and protozoans) within the marine food web has been recognized for several decades (Pomeroy, 1974). Bacterioplankton may account for a large sink of organic matter produced by primary producers, and the role of these microbes in determining the fate of organic carbon remains undetermined (Jahnke and Craven, 1995). Additionally, bacterial abundance (biomass) and activity (respiration) are not necessarily coupled. Determining the relationship of bacterial "abundance" and/or "activity" to factors such as autotrophic production and chlorophyll a is complicated. For instance, bacterial "activity" was more highly correlated to chlorophyll *a* than was bacterial biomass in the Oregon upwelling system (Sherr et al., 2001). Bacterial abundance was shown to decrease with increasing chlorophyll *a* concentration in Southern Ocean ecosystems (Bird and Karl, 1999; Karl and Bird, 1993). Studies showing a significant positive correlation between respiratory activity and chlorophyll *a* suggested that community respiration was dominated by photoautotrophs during the spring and summer seasons (Aristegui and Montero, 1995; Karl et al., 1991). In temperate coastal ecosystems, heterotrophic respiration may be temporally and, therefore, spatially decoupled from autotrophic production by a temporal lag (Blight et al., 1995; Robinson et al., 1999; Sherr and Sherr, 1996). Finally, a potential consequence of the high O_2 and low fCO_2 condition is the premature demise of the bloom via algal photorespiration, but there are very few, if any, estimates of photorespiration in Antarctic marine phytoplankton (Karl et al., 1996). Clearly, more work is needed to fully understand the controlling factors of heterotrophic respiration within the ecosystem.

Generally, DCR within Marguerite Bay remained low compared to NCP (Fig. 6B). The exception to this trend occurred at station within Marguerite Bay where NCP had essentially ceased. Although measured O_2 concentrations were above 450 μM and fCO_2 values were approximately 100 μatm, rates of DCR were greater than estimate of gross production (GP) implying net heterotrophy. Another anomalous station sampled in the ice covered area of Tickle Passage showed

high rates of DCR based on O_2 consumption but low rates based on production of CO_2.

At O_2 concentrations above 120% saturation, differential exchange of O_2 and CO_2 across the atmosphere-ocean interface decoupled oxygen and carbon dynamics. Oxygen produced was quickly ventilated to the atmosphere, whereas the CO_2 deficit in the upper water column remained. This caused an asymmetry in the gas fluxes and in the gas concentrations of the surface waters in these regions. The slope of $O_{2\{Sat\}}$ and $fCO_{2\{Sat\}}$ within Marguerite Bay had a significantly steeper slope of -3.8 (model II linear regression geometric mean) than was calculated for the entire Pal-LTER region (-0.7). This regression matched the ratio of $O_{2\{Sat\}}/fCO_{2\{Sat\}}$ for air–sea exchange at high O_2 concentrations (>400 μM). Because of air to sea exchange, O_2 concentrations decreased from 156% saturation to equilibrium (100% saturation) in approximately 30 days. The corresponding $fCO_{2\{Sat\}}$ increased only 9% within the same period. These differences in saturation states (56% for $O_{2\{Sat\}}$ versus 9% for CO_2) were largely a function of gas solubility. Consequently, we suggest that air-to-sea exchange was a major factor in returning O_2 values to their respective atmospheric equilibrium values in spite of measurable respiration. Due to differences in the behavior of these two biogenic gases, the same was not true for fCO_2 thus causing a decoupling in $O_{2\{Sat\}}/fCO_{2\{Sat\}}$ dynamics.

5. Conclusions

Heating and cooling of surface waters were relatively small sources and sinks (± 10–15% saturation relative to the atmosphere) of O_2 and CO_2 in the region west of the Antarctic Peninsula compared to net biological processes. Although heating and cooling were small sources and sinks, the spatial distribution of $O_{2\{Sat\}}/fCO_{2\{Sat\}}$ values centered around atmospheric equilibrium account for 80% of the Pal-LTER grid surveyed in January. The relative magnitude of net biological processes in changing O_2 and fCO_2 saturation states was approximately four-fold greater than for heating and cooling, yet occurs in only a small portion of the Pal-LTER grid surveyed. Because of variations in the time of air to sea exchange of CO_2 and O_2, excess oxygen returned to atmospheric equilibrium much more quickly than the replenishment of CO_2. Austral winter data collected in July confirmed that surface waters west of the Antarctic Peninsula were a local sink for O_2 and source of CO_2.

Acknowledgements

We thank the captains and crews of the *R/V Polar Duke* and the *RVIB Nathaniel B. Palmer*, and all of our colleagues who helped in the field. We would also

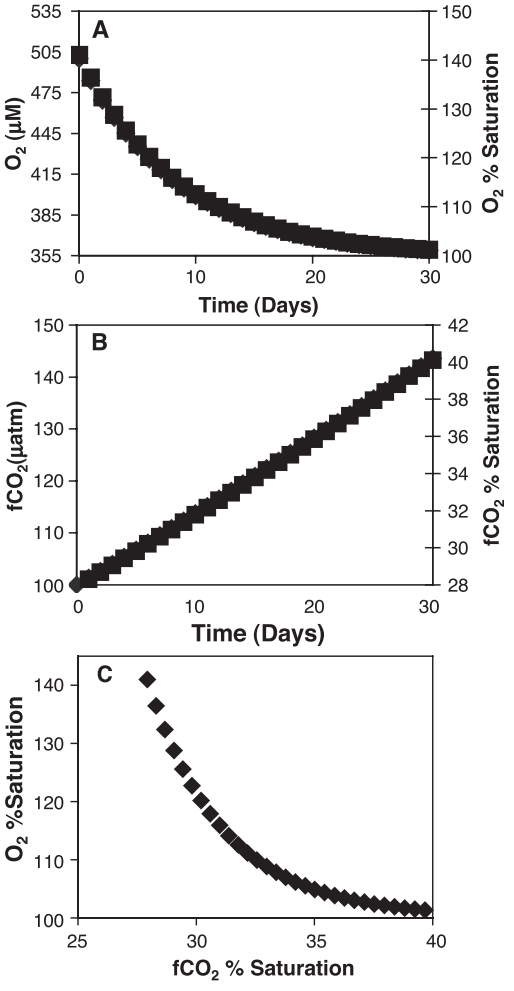


Fig. 7. (A) Changes in O_2 concentrations as a function of days based on air to sea exchange. (B) Changes in fCO_2 pressure as a function of days based on air to sea exchange. (C) Changes of % saturation of O_2 and fCO_2 based on air to sea exchange.

like to thank two anonymous reviewers for their helpful comments. This work was supported by NSF, Office of Polar Programs, Grant # OPP 96-32763. This is a Pal-LTER contribution 444.

Appendix A. Air–sea flux model

The difference between the air to sea exchange rates of O_2 and CO_2 can be illustrated by comparing modeled flux estimates. This is a model calculation and illustrates the different time-scales of O_2 and fCO_2 air–sea exchange. Modeled air–sea fCO_2 gas flux estimates were calculated by multiplying the atmosphere (358 μatm) and surface ocean fCO_2 difference by the gas transfer coefficient and solubility of CO_2 in seawater. The gas transfer coefficient was calculated using the equation of Wanninkhof (1992) with a constant wind speed of 3 m s^{-1}. The solubility of CO_2 in seawater was calculated from Weiss (1974). At each time step, fCO_2 is calculated from DIC using a Revelle factor of 15 (Takahashi et al., 1980b). Air–sea O_2 flux estimates were calculated using the equations of Weiss (1970) and the gas transfer coefficient. Model calculations were initiated with values of 1 °C, 33 salinity and concentrations of O_2, DIC and fCO_2 of 500 μM, 1900 μM and 100 μatm, respectively. The air–sea flux was calculated for every time step (1 day) and incremented.

Oxygen concentrations approach atmospheric equilibrium in approximately 30 days (Fig. 7A). In comparison, fCO_2 only changed by approximately 12% during the same time span (Fig. 7B). The change in the stoichiometric proportions of $O_{2\{Sat\}}$ and $fCO_{2\{Sat\}}$ decreased as O_2 and fCO_2 approach atmospheric equilibrium values (Fig. 7C). Oxygen concentrations approach atmospheric equilibrium concentrations much more quickly than CO_2 because of the lower solubility of O_2 versus fCO_2.

References

Alvarez, M., Rios, A.F., Roson, G., 2002. Spatio-temporal variability of air–sea fluxes of carbon dioxide and oxygen in the Bransfield and Gerlache Straits during austral summer 1995–96. Deep-Sea Research II 49, 643–662.

Aristegui, J., Montero, M., 1995. Plankton community respiration in Bransfield Strait (Antarctic Ocean) during austral spring. Journal of Plankton Research 17, 1647–1659.

Bender, M., Ellis, T., Tans, P., Francey, R., Lowe, D., 1996. Variability in the O_2/N_2 ratio of southern hemisphere air, 1991–1994: implications for the carbon cycle. Global Biogeochemical Cycles 10, 9–21.

Bender, M.L., Dickson, M.-L., Orchardo, J., 2000. Net and gross production in the Ross Sea as determined by incubation experiments and dissolved O_2 studies. Deep-Sea Research II 47, 3141–3158.

Bird, D.F., Karl, D.M., 1999. Uncoupling of bacteria and phytoplankton during the austral spring bloom in Gerlache Strait, Antarctic Peninsula. Aquatic Microbial Ecology 19, 13–27.

Bjork, V.O., 1948. Brain perfusions in dogs with artificially oxygenated blood. Acta Chirurgica Scandinavica Supplementum 96, 9–122.

Blight, S.B., et al., 1995. Phasing of autotrophic and heterotrophic plankton metabolism in a temperate coastal ecosystem. Marine Ecology Progress Series 128, 61–75.

Broecker, W.S., Peng, T.-H., 1982. Tracers in the Sea. Lamont-Doherty Geological Observatory, New York.

Calderia, K., Philip, D.B., 2000. The role of the Southern Ocean in uptake and storage of anthropogenic carbon dioxide. Science 287, 620.

Carrillo, C.J., 2002. Processes controlling carbon dioxide in seawater. PhD thesis, University of Hawaii, Honolulu, HI.

Carrillo, C.J., Karl, D.M., 1999. Dissolved inorganic carbon pool dynamics in northern Gerlache Strait, Antarctica. Journal of Geophysical Research 104, 15873–15884.

Cross, F.S., Berne, R.M., Hirose, Y., Jones, R.D., Kay, E.B., 1956. Evaluation of a rotating type reservoir-oxygenator. Proceedings Society of Experimental Biology and Medicine 93, 210–214.

DeGrandpre, M.D., Hammar, T.R., Wallace, D.W.R., Wirick, C.D., 1997. Simultaneous mooring-based measurements of seawater CO_2 and O_2 off Cape Hatteras, North Carolina. Limnology and Oceanography 42, 21–28.

DeGrandpre, M.D., Hammar, T.R., Wirick, C.D., 1998. Short-term pCO_2 and O_2 dynamics in California coastal waters. Deep-Sea Research II 45, 1557–1575.

Dierssen, H.M., Smith, R.C., Vernet, M., 2002. Glacial meltwater dynamics in coastal waters west of the Antarctic peninsula. PNAS 99, 1790–1795.

DOE, 1994. Handbook of methods for the analysis of the various parameters of the carbon dioxide system in seawater; version 2. ORNL/CDIAC-74.

Gordon, A.L., Huber, B.A., 1990. Southern Ocean winter mixed layer. Journal of Geophysical Research 95, 11655–11672.

Goyet, C., Millero, F.J., Poisson, A., Shafer, D.K., 1993. Temperature dependence of CO_2 fugacity in seawater. Marine Chemistry 44, 205–219.

Hofmann, E.E., Klinck, J.M., Lascara, C.M., Smith, D.A., 1996. Water mass distribution and circulation west of the Antarctic Peninsula and including Bransfield Strait. In: Ross, R.M., Hofmann, E.E., Quetin, L.B. (Eds.), Foundations for Ecological Research West of the Antarctic Peninsula. American Geophysical Union, Washington, pp. 61–80.

Holm-Hansen, O., Mitchell, B.G., 1991. Spatial and temporal dis-

tribution of phytoplankton and primary production in the western Bransfield Strait region. Deep-Sea Research 38, 961–980.

Holm-Hansen, O., Mitchell, B.G., Hewes, C.D., Karl, D.M., 1989. Phytoplankton blooms in the vicinity of Palmer Station, Antarctica. Polar Biology 10, 49–57.

Jahnke, R.A., Craven, D.B., 1995. Quantifying the role of heterotrophic bacteria in the carbon cycle: a need for respiration rate measurements. Limnology and Oceanography 40, 436–441.

Johnson, K.M., Williams, P.J.leB., Brandstorm, L., Sieburth, J.M., 1987. Coulometric TCO_2 analysis for marine studies: automation and calibration. Marine Chemistry 21, 117–133.

Kanwisher, J., 1963. On the exchange of gases between the atmosphere and the sea. Deep-Sea Research 10, 195–207.

Karl, D.M., Bird, D.F., 1993. Bacterial-agal interactions in Antarctic coastal ecosystems. In: Pedros-Alio, G.E. (Ed.), Trends in Microbial Ecology, Sixth International Symposium on Microbial Ecology, pp. 37–40.

Karl, D.M., Holm-Hansen, O., Taylor, G.T., Tien, G.T., Bird, D.F., 1991. Microbial biomass and productivity in the western Bransfield Strait, Antarctica during the 1986–87 austral summer. Deep-Sea Research 38, 1029–1055.

Karl, D.M., Christian, J.R., Dore, J.E., Letelier, R.M., 1996. Microbiological oceanography in the region west of the Antarctic peninsula: microbial dynamics, nitrogen cycle and carbon flux. In: Ross, R.M., Hofmann, E.E., Quetin, L.B. (Eds.), Foundations for Ecological Research West of the Antarctic Peninsula. American Geophysical Union, Washington, pp. 303–332.

Keeling, R.F., Shertz, S.R., 1992. Seasonal and interannual variations in atmospheric oxygen and implications for global carbon cycle. Nature 358, 723–727.

Keeling, R.F., Najjar, R.P., Bender, M.L., Tans, P.P., 1993. What atmospheric oxygen measurements can tell us about the global carbon cycle. Global Biogeochemical Cycles 7, 37–67.

Klinck, J.M., 1998. Heat and salt changes on the continental shelf west of the Antarctic Peninsula between January 1993 and January 1994. Journal of Geophysical Research 103, 7617–7636.

Laws, E.A., 1991. Photosyntheic quotients, new production and net community production in the open ocean. Deep-Sea Research 38, 143–167.

Liss, P.S., Merlivat, L., 1986. Air–sea gas exchange rates: introduction and synthesis. The Role of Air–Sea Exchange in Geochemical Cycling. D. Reidel, Hingham, MA, pp. 113–129.

Moore, J.K., Abott, M.R., Richman, J.R., Smith, W.O., Cowles, T.J., Coale, K.H., Gardner, W.D., Barber, R.T., 1999. SeaWiFS satellite ocean color data from the Southern Ocean. Geophysical Research Letters 26, 1465–1468.

Ohshima, K.I., Yoshida, K., Shimoda, H., Wakatsuchi, M., Endoh, T., Fukuchi, M., 1998. Relationship between the upper ocean and sea ice during the Antarctic melting season. Journal of Geophysical Research 103, 7601–7615.

Pomeroy, L.R., 1974. The ocean's food web, a changing paradigm. Bioscience 24, 499–504.

Robinson, C., Archer, S.D., Williams, P.J.leB., 1999. Microbial dynamics in coastal waters of East Antarctica: plankton production and respiration. Marine Ecology Progress Series 180, 23–36.

Ross, R.M., Quetin, L.B., Baker, K.S., Vernet, M., Smith, R.C., 2000. Growth limitation in young euphausia superba. Limnology and Oceanography 45, 31–43.

Sabine, C.L., Key, R.M., 1998. Controls on fCO_2 in the South Pacific. Marine Chemistry 60, 95–110.

Sabine, C.L., et al., 1999. Anthropogenic CO_2 inventory of the Indian Ocean. Global Biogeochemical Cycles 13, 179–198.

Schink, D.R., Sigalove, J.J., Charnell, R.L., Guinasso Jr., N.L., 1970. Use of Rn/Ra ratios to determine air/sea gas exchange and vertical mixing in the sea, a final technical report. Office of Naval Research, Palo Alto.

Sherr, E.B., Sherr, B.F., 1996. Temporal offset in oceanic production and respiration processes implied by seasonal changes in atmospheric oxygen: the role of heterotrophic microbes. Aquatic Microbial Ecology 11, 91–100.

Sherr, E.B., Sherr, B.F., Cowles, T.J., 2001. Mesoscale variability in bacterial activity in the Northwest Pacific off Oregon, USA. Aquatic Microbial Ecology 25, 21–30.

Simpson, J.J., 1985. Air–sea exchange of carbon dioxide and oxygen induced by phytoplankton. Mapping Strategies in Chemical Oceanography. The Society, Washington D.C., pp. 409–450.

Smith, S.V., 1985. Physical, chemical and biological characteristics of CO_2 gas flux across the air-water interface. Plant, Cell and Environment 8, 387–398.

Smith, W.O., Nelson, D.M., 1985. Phytoplankton bloom produced by a receding ice edge in the Ross Sea: spatial coherence with the density field. Science 227, 163–166.

Smith, R.C., Baker, K.S., Dustan, P., 1981. Fluorometric Techniques for the Measurement of Oceanic Chlorophyll in the Support of Remote Sensing. SIORef. 81-17. Scripps Institution of Oceanography, University of California San Diego, La Jolla.

Smith, R.C., Booth, C.R., Star, J.L., 1984. Oceanographic bio-optical profiling system. Applied Optics 23, 2791–2797.

Smith, R.C., et al., 1995. The Palmer LTER: a long-term ecological research program at Palmer Station, Antarctica. Oceanography Magazine 8, 77–86.

Smith, R.C., Dierssen, H.M., Vernet, M., 1996. Phytoplankton biomass and productivity in the western Antarctic Peninsula Region. In: Ross, R.M., Hofmann, E.E., Quetin, L.B. (Eds.), Foundations for Ecological Research West of the Antarctic Peninsula. American Geophysical Union, Washington, DC, pp. 333–356.

Smith, D.A., Hofmann, E.E., Klinck, J.M., Lascara, C.M., 1999a. Hydrography and circulation of the West Antarctic Peninsula Continental Shelf. Deep-Sea Research 46, 925–949.

Smith, R.C., et al., 1999b. Marine ecosystem sensitivity to climate change. Bioscience 49, 393–404.

Smith, R.C., Baker, K.S., Dierssen, H.M., Stammerjohn, S.E., Vernet, M., 2001. Variability of primary production in an Antarctic marine ecosystem as estimated using a multi-scale sampling strategy. Am. Zool. 41, 40–56.

Takahashi, T., Broecker, W.S., Werner, S.R., Bainbridge, A.E., 1980a. Carbonate chemistry of the surface waters of the world oceans. In: Goldberg, E.D., Horibe, Y., Saruhashi, K. (Eds.), Isotope Marine Chemistry. Uchida Rokakuko, Tokyo, pp. 291–326.

Takahashi, T., Broecker, W.S., Werner, S.R., Brainbridge, A.E.,

1980b. Carbonate chemistry of the surface waters of the world oceans. In: Saruhashi, K. (Ed.), Isotope Marine Chemistry. Uchida Rokakuko, Tokyo, pp. 291–325.

Takahashi, T., Olafsson, J., Goddard, J.G., Chipman, D.W., Sutherland, S.C., 1993. Seasonal variation of CO_2 and nutrients in high latitude surface oceans: a comparative study. Global Biogeochemical Cycles 7, 843–878.

Tomczak, M., Godfrey, S.J., 1994. Regional Oceanography: An Introduction. Pergamon, Tarrytown, New York.

van Geen, A., Takesue, R.K., Goddard, J., Takahashi, T., Barth, J.A., Smith, R.L., 2000. Carbon and nutrient dynamics during coastal upwelling off Cape Blanco, Oregon. Deep-Sea Research II 47, 975–1002.

Volk, T., Hoffert, M.I., 1985. Ocean carbon pumps: analysis of relative strengths and efficiencies in ocean-driven atmospheric CO_2 changes. Natural Variations Archean to Present, vol. 32. American Geophysical Union, Washington, DC, pp. 99–110.

Wanninkhof, R., 1992. Relationship between wind speed and gas exchange over the ocean. Journal of Geophysical Research 97, 7373–7382.

Waters, K.J., Smith, R.C., 1992. Palmer LTER: a sampling grid for the Palmer LTER program. Antarctic Journal of the United States 27, 236–239.

Weiss, R.F., 1970. The solubility of nitrogen, oxygen and argon in water and seawater. Deep-Sea Research 17, 721–735.

Weiss, R.F., 1974. Carbon dioxide in water and seawater: the solubility of a non-ideal gas. Marine Chemistry 2, 203–215.